FSU-HEP-961001
hep-ph/9610224

QCD IMPROVED $b \to s\gamma$ CONSTRAINTS ON THE MINIMAL SUPERGRAVITY MODEL

Howard Baer and Michal Brhlik
Department of Physics, Florida State University, Tallahassee, FL 32306 USA
(February 1, 2008)

arXiv:hep-ph/9610224v2 14 Oct 1996

Abstract

Recent advances in the QCD corrections to $b \to s\gamma$ decay in the MSSM include *i.*) evaluation of the relevant operators, Wilson coefficients and anomalous dimension matrix elements for the various MSSM effective theories valid at scales beyond $Q = M_W$, *ii.*) calculations of most of the needed anomalous dimension matrix elements to next-to-leading order for scales $m_b \lesssim Q < M_W$, and *iii.*) calculations of $\mathcal{O}(\alpha_s)$ virtual and bremsstrahlung corrections to the $b \to s\gamma$ decay operators at scale $Q \sim m_b$. We assemble all these known results to gain an estimate of $B(b \to s\gamma)$ for the parameter space of the minimal supergravity model (mSUGRA). We find a much reduced scale dependence of our result compared to usual leading-log evaluations. Comparison with the latest CLEO results yields stringent constraints on parameter space. Much of mSUGRA parameter space is ruled out for $\mu < 0$, especially for large $\tan\beta$. We compare these results with other constraints from cosmology and non-standard vacua. Also, we compare with expectations for discovering mSUGRA at LEP2, the Tevatron and the CERN LHC.

Typeset using REVTEX

I. INTRODUCTION

Particle physics models including weak-scale supersymmetry (SUSY) are amongst the most compelling candidates [1] for physics beyond the Standard Model (SM). Of this class of models, the minimal supergravity model (mSUGRA) stands out as at least the most popular framework for performing searches for SUSY, and can justifiably be called the paradigm model for weak scale supersymmetry [2]. The mSUGRA model can be characterized briefly by the following attributes [3,2]:

- particle content and gauge symmetries of the Minimal Supersymmetric Standard Model (MSSM), *i.e.* a supersymmetrized version of the two-Higgs doublet SM, plus all allowed soft SUSY breaking terms,
- a desert between the weak scale and the unification scale, which allows for gauge coupling unification,
- universal boundary conditions for soft-SUSY breaking terms $m_0,\ m_{1/2},\ A_0$ and B_0 implemented at the unification scale M_X,
- electroweak symmetry is broken radiatively, and is a consequence of the large top quark Yukawa coupling.

The various weak scale parameters are related to GUT scale parameters via renormalization group equations (RGE's). Typically, all weak-scale sparticle masses and mixings are then determined by the parameter set

$$m_0,\ m_{1/2},\ A_0,\ \tan\beta \text{ and } sign(\mu), \tag{1.1}$$

along with the measured value of m_t. We take $m_t = 170$ GeV throughout this paper.

Of course, not all values of the above parameter set are allowed. For some values, electroweak symmetry is not broken appropriately. For other values, a charged or colored sparticle may be the lightest SUSY particle (LSP), in conflict with cosmology and searches for exotic nuclei and atoms. In addition, there exist constraints from negative searches for sparticles at the Fermilab Tevatron $p\bar{p}$ and LEP2 e^+e^- colliders. In particular, we note the recent bound that $m_{\widetilde{W}_1} > 79$ GeV for a gaugino-like lightest chargino [4]. Additionally, in the absence of R-violating interactions, there exist bounds on parameter space from the relic density of neutralinos produced in the Big Bang [5]; for certain regions of parameter space, the neutralino relic density $\Omega h^2 > 1$, which implies a universe younger than 10 billion years, in contradiction at least with the ages of the oldest stars in globular clusters. Finally, several recent papers have mapped out regions of mSUGRA parameter space where there exist vacua deeper than the standard minimum [6]. These non-standard vacua constraints may not be rigorous, however, if one entertains the notion that the universe may have settled into a false vacuum.

The parameter space of the mSUGRA model (as well as many other models [7]) may also be constrained by data from rare meson decays, such as the branching fraction for $B \to X_s\gamma$. A recent analysis by the CLEO collaboration finds for the inclusive decays $B(B \to X_s\gamma) = (2.32 \pm 0.67) \times 10^{-4}$, with 95% CL upper and lower limits (including systematic errors) of 4.2×10^{-4} and 1×10^{-4}, respectively [8]. Such data, when compared

against theoretical predictions of $b \to s\gamma$, have been shown to be very restrictive for both two-Higgs doublet models (2HDM) [9] and supersymmetric models [10,11]. For a type II 2HDM, loop contributions involving the top quark and charged Higgs $H^{\pm}$ add constructively with SM loops involving top and W bosons. In the MSSM, there exist other contributions involving squark-chargino loops, squark-neutralino loops, and squark-gluino loops. The latter two contributions are much smaller than squark-chargino loop contributions, and are frequently neglected. The squark-chargino loop contribution can add either constructively or destructively with the W and H^+ loops, leading to allowed or forbidden regions of SUSY model parameter space.

These calculations are usually performed by evaluating lowest order matrix elements of effective theory operators at a scale $Q \sim m_b$. All orders approximate QCD corrections are included via renormalization group resummation of leading logs (LL) which arise due to a disparity between the scale at which new physics enters the $b \to s\gamma$ loop corrections (usually taken to be $Q \sim M_W$), and the scale at which the $b \to s\gamma$ decay rate is evaluated ($Q \sim m_b$). The resummation is most easily performed within the framework of effective field theories. Above the scale $Q = M_W$ (all scales $Q \sim M_W$ are equivalent in LL perturbation theory), calculations are performed within the full theory. Below $Q = M_W$, heavy particles are integrated out of the theory, leading to an effective Hamiltonian

$$H_{eff} = -\frac{4G_F}{\sqrt{2}} V_{tb} V_{ts}^* \sum_{i=1}^{8} C_i(Q) O_i(Q), \tag{1.2}$$

where matching between the two theories occurs at $Q = M_W$ and yields the values of $C_i(Q = M_W)$. In Eq. 1.2, the $C_i(Q)$ are Wilson coefficients evaluated at scale Q, and the O_i are a complete set of operators, given, for example, in Ref. [12]. Resummation then occurs by solving the renormalization group equations (RGE's) for the Wilson coefficients

$$Q\frac{d}{dQ} C_i(Q) = \gamma_{ji} C_j(Q), \tag{1.3}$$

where γ is the 8×8 anomalous dimension matrix (ADM), and

$$\gamma = \frac{\alpha_s}{4\pi}\gamma^{(0)} + (\frac{\alpha_s}{4\pi})^2 \gamma^{(1)} + \ldots. \tag{1.4}$$

The matrix elements of the operators O_i are finally calculated at a scale $Q \sim m_b$ and multiplied by the appropriately evolved Wilson coefficients to gain the final decay amplitude.

The LL QCD corrections just described yield enhancements in the $b \to s\gamma$ decay rate of factors of $2 - 5$ [13,14]. The resulting LL calculation yields an answer which is ambiguous depending upon which precise scale choice is chosen for evaluation of matrix elements of the operators O_i. Variation of the scale $\frac{m_b}{2} < Q < 2m_b$ yields approximately a 25% uncertainty in the theoretical calculation. This uncertainty provides the greatest source of error in currently available theoretical calculations [14]. To reduce the theoretical uncertainty, one must proceed to a next-to-leading-log calculation (NLL) of the $b \to s\gamma$ decay rate.

Recently, a number of theoretical developments have been made towards the goal of a NLL calculation of $B(b \to s\gamma)$. Cho and Grinstein showed [15] that if there are two significantly different masses contributing to the loop amplitude (such as m_t and M_W), then in fact there can already exist significant corrections to the Wilson coefficients at scale M_W.

In this case, one must create an effective theory by first integrating out the heavy top quark, apply RGE running between the scales m_t and M_W, and then integrate out the W boson to arrive at the operator set in 1.2. The above procedure gives a $\sim 20\%$ enhancement to the SM value of $B(b \to s\gamma)$. In supersymmetric models, many more heavy particles are present. Anlauf has shown how to perform a similar analysis for the case of the MSSM [16]. These corrections are considered to be next-to-leading order effects.

In addition, various terms of the ADM in Eq. 1.4 have been calculated to next-to-leading order (NLO). The $\mathcal{O}(\alpha_s^2)$ terms $\gamma_{ij}^{(1)}$ for $i,j = 1-6$ have been calculated by Ciuchini *et. al.* [17], while the corresponding terms for $i,j = 7,8$ are given by Misiak and Münz [18]. Of the remaining terms which mix the $i = 1-6$ and $j = 7,8$ Wilson coefficients, only $\gamma_{27}^{(1)}$ is relevant, but its evaluation requires a three loop calculation. A preliminary report on the calculation of $\gamma_{27}^{(1)}$ indicates that it is only a small effect [19].

Finally, the QCD corrections to the operators O_i must be included [20,21]. Recently, Greub, Hurth and Wyler have reported results [21] on the complete virtual corrections to the relevant operators O_2, O_7 and O_8. Combining these with the bremsstrahlung corrections [22,21] results in cancellation of associated soft and collinear singularities. A combination of the QCD corrected operator matrix elements $< s\gamma|O_i|b >$ with the complete $\mathcal{O}(\alpha_s)$ corrected Wilson coefficients at scale $Q \sim m_b$ will result in a NLL calculation of the $B(b \to s\gamma)$ decay rate.

In this paper, we have nothing new to add to the calculational procedure for evaluating $B(b \to s\gamma)$. Our goal in this paper is to bring together the above pieces of a NLL calculation of $B(b \to s\gamma)$ and to interface with the mSUGRA model so that detailed comparisons to data can be made in parameter space. In so doing, we simply neglect the missing piece of the calculation, $\gamma_{27}^{(1)}$. This will result in some small scheme dependence of our results, and in some additional scale dependence, so our calculation will not be truly NLL. Hence, we label it as QCD improved, in hope that $\gamma_{27}^{(1)}$ turns out small, as preliminary reports suggest.

Our goal as well is to evaluate the $B(b \to s\gamma)$ rate as a function of mSUGRA parameters and compare with the recent CLEO results, to find favored or excluded regions of parameter space. We find the $b \to s\gamma$ constraint to be really very strong, as noted previously [10,11]. We compare the $b \to s\gamma$ results to other recent results on relic density constraints [5] and regions of non-standard vacua [6]. Finally, we note the effect of $B(b \to s\gamma)$ on expectations for discovering mSUGRA at various collider experiments. Toward these ends, in Sec. 2 we present various details of our QCD improved calculation for $B(b \to s\gamma)$. In Sec. 3, we report on our results as a function of mSUGRA parameter space, and compare with other constraints and expectations for collider searches. We summarize in Sec. 4.

II. CALCULATIONAL METHOD

In this section, we outline our procedure for calculating $B(b \to s\gamma)$ as a function of mSUGRA parameter space. Our first step of course is to input the parameter set 1.1 and solve for the superparticle masses and mixings via running of the mSUGRA RGE equations between M_Z and M_{GUT} and imposing the appropriate minimization criteria using the 1-loop corrected effective potential. We iterate the running back and forth between the two scales six times using the usual Runge-Kutta method; this results in a convergent spectrum of superparticle masses. The procedure is described more fully in Ref. [23]. On the last run

down but one, we take note of the various superparticle masses. On the final run from M_{GUT} to M_Z, we implement the procedures outlined in Anlauf [16] to ultimately obtain the needed Wilson coefficients $C_7(M_W)$ and $C_8(M_W)$. In addition, the values of $C_i(M_W)$ for $i = 1 - 6$ are given in Ref. [17] to $\mathcal{O}(\alpha_s)$.

Given a heavy particle of mass m_H and a light particle of mass m_L contributing to a $b \to s\gamma$ loop, the procedure of Anlauf is as follows. First, at scale $Q = m_H$, the heavy particle is decoupled from the theory and the corresponding effective field theory is constructed. The leading terms of the expansion of C_i in terms of $x = (\frac{m_L}{m_H})^2$ are calculated and evolved to scale $Q = m_L$ using the ADM including both QCD and electroweak interactions. Taking only leading terms in x restricts the operator basis to dimension 5 and 6 operators [16]. At $Q = m_L$, the remaining part of C_i, which has been evolved down to m_L using only the EW ADM, is added together with eventual contributions coming from decoupling of the lighter particle in the loop. As a last step, the equations of motion are applied to obtain $C_7(M_W)$ and $C_8(M_W)$. In the case that $m_L < M_W$, the evolution is stopped at M_W. In practise, this is almost never a problem, in light of the new bound $m_{\widetilde{W}_1} > 79$ GeV for gaugino-like charginos from LEP2. In our calculation, we include contributions from tW, tH^- and $\widetilde{W}_i\tilde{q}_j$ loops, for $i = 1$ and 2, and $\tilde{q}_j = \tilde{u}_L,\ \tilde{u}_R,\ \tilde{c}_L,\ \tilde{c}_R,\ \tilde{t}_1$ and $\tilde{t}_2$, and neglect contributions from $\widetilde{Z}_i\tilde{q}_j$ and $\tilde{g}\tilde{q}_j$ loops, which should have much smaller contributions.

As an illustration of these results, we show in Fig. 1 the final value of the Wilson coefficient $C_7(M_W)$ from the various loop contributions just discussed, as a function of $m_{1/2}$, where $m_0 = m_{1/2}$, $\tan\beta = 2$ and $A_0 = 0$. In frame *a*) $\mu < 0$, while in frame *b*), $\mu > 0$. The tW SM contribution is just $\simeq -0.23$, and of course doesn't vary versus SUSY soft-breaking parameters. In both frames, the tH^- contribution is negative, and decreases in absolute value as $m_{1/2}$ increases, since the value of m_{H^-} is increasing. Note this contribution adds constructively to the SM tW contribution; when combined, these give the large constraints on type II 2HDM's [9]. For $\mu < 0$, most of the SUSY particle loop contributions are also negative in this case, which leads to the significant constraints to be given in Sec. 3. The exceptions are the large positive contributions from $\widetilde{W}_2\tilde{t}_2$ and $\widetilde{W}_1\tilde{q}$, which cancel some of the large negative contributions. Alternatively, for $\mu > 0$, we see in frame *b*) that there are several positive as well as negative contributions to $C_7(M_W)$. In this case, one can achieve rates for $B(b \to s\gamma)$ which are equal to or even smaller than the SM value.

The next step in our calculation is to implement the NLO ADM to calculate the running of the C_i's from M_W down to $Q \sim m_b$. The terms $\gamma_{ij}^{(1)}$ for $i, j = 1 - 6$ have been calculated in Ref. [17]. The corresponding ADM elements for $i, j = 7, 8$ have been calculated in Ref. [18]. The remaining NLO ADM elements for $\gamma_{ij}^{(1)}$ for $i = 1 - 6$ and $j = 7, 8$ have not yet been published. The most important of these is $\gamma_{27}^{(1)}$, since $C_2(M_W) \simeq 1$ while the remaining $C_i(M_W)$ which mix into C_7 are ~ 0 [21]. Preliminary results of the three-loop calculation of $\gamma_{27}^{(1)}$ indicate it is small [19], so in our calculation, we take $\gamma_{27}^{(1)} = 0$.

We show in Fig. 2 the evolution of the set of Wilson coefficients C_i for $i = 1 - 8$, from their values at $Q = M_W$ down to $Q = 1$ GeV. Frame *a*) shows the evolution including just LO terms in the ADM, while frame *b*) includes the NLO ADM contributions mentioned above. We see that in general, the NLO effects are small. The exception is for C_7, for which the NLO correction differs from LO by $\sim 10\%$.

Finally, we must include the matrix elements $< s\gamma|O_i(Q)|b >$ at NLO. We neglect the O_3, O_4, O_5 and O_6 contributions, since the corresponding C_i are small, as shown in Fig.

2. Furthermore, the matrix element $< s\gamma|O_1|b >$ is exactly zero. The bremsstrahlung graphs have been calculated in Ref. [22] for $b \to s\gamma g$, while the complete virtual corrections to the operators O_2, O_7 and O_8 have been calculated in Ref. [21]. We implement these results, which ensure the proper cancellation of infrared and collinear singularities. Since our final results are not completely NLL, we will have some remaining scheme dependence. All our calculations have been performed within the naive dimensional regularization (NDR) scheme, in which the calculational building blocks have been given. We neglect throughout our calculation any long distance effects [24] on the $b \to s\gamma$ decay rate.

Our final numerical result is given by

$$B(b \to s\gamma) = \frac{\Gamma}{\Gamma_{sl}} B_{sl}, \tag{2.1}$$

where

$$\Gamma(b \to s\gamma) = \Gamma_{virt} + \Gamma_{brem}. \tag{2.2}$$

In the above, Γ_{virt} is given by Eq. (5.6) of Ref. [21], and Γ_{brem} is given in Ref. [22,21], while Γ_{sl} is given by Eq. (5.9) of Ref. [21]. Numerically, we take the combination $\frac{V_{ts}^* V_{tb}}{|V_{cb}|^2} = 0.95$ and $B_{sl} = 0.104$.

The inclusion of the various above mentioned QCD improvements leads to a result for $B(b \to s\gamma)$ which has significantly reduced scale-dependence. We illustrate the scale dependence of our result in Fig. 3, where we plot $B(b \to s\gamma)$ versus Q, where $\frac{m_b}{2} < Q < 2m_b$. The LL calculation for the SM value is denoted by the dashed curve, which yields $B(b \to s\gamma) = 2.9 \pm 0.7$, or a 25% uncertainty due to scale choice. The QCD-improved result is shown by the solid curve. In this case, the prediction is $B(b \to s\gamma) = 3.2 \pm 0.3$, and the error due to scale choice uncertainty is reduced to $\sim 9\%$. The CLEO measured central value is denoted by the solid horizontal line. The 1σ limits are denoted by dotted lines, and the 95% CL limits are denoted by solid lines. We see that the SM prediction lies somewhat above the CLEO measured result, although it is well within the 95% CL region.

III. NUMERICAL RESULTS AND IMPLICATIONS

A. Results for $B(b \to s\gamma)$

We present our main results on the $b \to s\gamma$ branching ratio as contours of constant branching fraction in the m_0 *vs.* $m_{1/2}$ plane. This allows a direct comparison of previous work on mSUGRA constraints and also collider expectations to be made with the present work. In Fig. 4, we show the $B(b \to s\gamma)$ contours for $A_0 = 0$ for *a*) $\tan\beta = 2,\ \mu < 0$, *b*) $\tan\beta = 2,\ \mu > 0$, *c*) $\tan\beta = 10,\ \mu < 0$ and *d*) $\tan\beta = 10,\ \mu > 0$. Each contour must be multiplied by 10^{-4}. The values of $B(b \to s\gamma)$ shown are for $Q = m_b$. The regions marked TH are excluded by theoretical constraints: either the lightest SUSY particle (LSP) is not the neutralino $\widetilde{Z}_1$, or electroweak symmetry is improperly broken. The regions marked EX are excluded by negative SUSY particle search experiments at Fermilab Tevatron or LEP. The new bound on $m_{\widetilde{W}_1} > 79$ GeV on gaugino-like charginos from LEP2 is indicated by the dashed contour.

In frame *a*), we find $B(b \to s\gamma)$ to be large for small values of m_0 and $m_{1/2}$. This is due to constructive interference amongst many of the SUSY and SM loop contributions, as can be gleaned from Fig. 1*a*. As m_0 and $m_{1/2}$ increase, the SUSY particles and charged Higgs boson all increase in mass, and their loop contributions become small: thus the value of $B(b \to s\gamma)$ gradually approaches its SM value in the upper-right region of each frame. We note the CLEO 95% CL upper bound on the inclusive rate for $B(b \to s\gamma)$ is 4.2×10^{-4}, so it becomes evident that a significant region to the lower-left of frame *a*) will become excluded. In frame *b*), for $\mu > 0$, the results are significantly different. In this case, there are many interfering loop contributions (see Fig. 1*b*), so the $B(b \to s\gamma)$ rate is much closer to the SM value, and can even drop below it. Since all the contours lie within the CLEO 95% excluded band, this frame remains unconstrained by $B(b \to s\gamma)$. For frame *c*), with $\tan\beta = 10$ and $\mu < 0$, we find very large values of $B(b \to s\gamma)$ throughout the entire region of the plane shown. Almost all of the plane shown gives values of $B(b \to s\gamma)$ greater than the CLEO 95% CL bound, and so will be excluded. Values of $m_{1/2} \gtrsim 500$ GeV are required to reach an allowed region for this choice of mSUGRA parameters. Finally, in frame *d*), we show the $B(b \to s\gamma)$ result for $\tan\beta = 10$ and $\mu > 0$. As in frame *b*), there exists substantial interference amongst the various loop contributions. The interference in this case is so great that a large fraction of the plane actually has $B(b \to s\gamma)$ values *below* the SM value. The $B(b \to s\gamma)$ rate increases with $m_{1/2}$ to reach its SM value.

Fig. 4 showed results for the GUT scale trilinear coupling $A_0 = 0$. Changing the value of A_0 will change the weak scale A parameters, which can result in changes to the top squark mass matrix and mixing angles. This can then affect the $\widetilde{W}_i\tilde{t}_j$ loop contributions. To show the effect of changing A_0, we show in Fig. 5 the $B(b \to s\gamma)$ contours in the m_0 *vs.* A_0 plane, for fixed $m_{1/2} = 200$ GeV, and all other parameters as in Fig. 4. There are some small TH excluded regions in the left-hand corners of the $\tan\beta = 2$ frames. In frame *a*), we see that the $B(b \to s\gamma)$ rate varies mainly with m_0 rather than A_0, and that only a small portion of the plane is above the CLEO 95% excluded value of $B(b \to s\gamma) = 4.2 \times 10^{-4}$. In frame *b*), the $B(b \to s\gamma)$ rate varies slowly versus parameters, and the entire plane shown is allowed. Frame *c*) again varies slowly with A_0, and is entirely exluded. Frame *d*) has significant variation against parameters, but is still entirely allowed.

B. Relationship to Other Constraints on the mSUGRA Model

Our next task is to compare the constraints from $b \to s\gamma$ with other constraints, and derive conclusions relevant for collider searches. Towards this end, we show in Fig. 6 regions of the m_0 *vs.* $m_{1/2}$ plane which are excluded by CLEO data on $B(b \to s\gamma)$ at 95% CL. We match against the theoretical result from this paper. To obtain the excluded region, the $B(b \to s\gamma)$ rate must fall outside the CLEO allowed values for *all* scale choices $\frac{m_b}{2} < Q < 2m_b$. The relevant excluded region for frame *a*) lies to the lower-left of the solid contour labelled $b \to s\gamma$. We show as well the dashed contour, below which $m_{\widetilde{W}_1} < 79$ GeV, in violation of recent LEP2 chargino searches [4]. The region to the left of the line of open circles is where non-standard minima of the mSUGRA model scalar potential lie [6]. This region may not be truly constrained if one is willing to accept that our universe may have settled into a false vacuum. The region to the right of the solid contour labelled by Ωh^2 is excluded by cosmological considerations [5]. In R-conserving models where the

lightest neutralino is the LSP, it can be an excellent candidate to make up the bulk of the dark matter of the universe. Such a cold dark matter (CDM) particle would have been produced in abundance in the early universe, and their present day abundance can then be straightforwardly calculated. If the relic density is too high, then the calculated lifetime of the universe is too short to be consistent with various astrophysical observations. The contour denoted by Ωh^2 denotes where the relic density $\Omega h^2 = 1$; for higher values of Ωh^2, the universe would be younger than 10 billion years old, and so is certainly excluded. In addition, a number of cosmological observations (COBE data, nuclear abundances, large scale structure) favor a universe formed with a 2:1 ratio of CDM to hot dark matter (HDM-*e.g.* neutrinos). This is called the mixed dark matter scenario (MDM). This cosmologically favored region lies between the dot-dashed contours, for which $0.15 < \Omega h^2 < 0.4$.

We combine the above mentioned constraints all on one plot, as in Fig. 6. We see that in frame *a*), if one combines the false vacua region with the $B(b \to s\gamma)$ constraint, much of the cosmologically favored MDM region is ruled out! Recent calculation of parameters associated with fine-tuning in the mSUGRA model [25] actually prefer the small m_0 and $m_{1/2}$ regions that are excluded by $B(b \to s\gamma)$ in this case.

In frame *b*) of Fig. 6, the entire region shown is allowed by $B(b \to s\gamma)$, and in fact would be favored over the frame *a*) results by the CLEO central value, which lies somewhat below the SM $B(b \to s\gamma)$ prediction. Meanwhile, much of the region shown in frame *c*) is excluded by $b \to s\gamma$, including all of the cosmological MDM prefered region. Finally, in frame *d*), the entire region is allowed by $B(b \to s\gamma)$. In fact, in this case, the region around $m_{1/2} \sim 200$ GeV actually agrees with the central value of the CLEO measurement of $B(b \to s\gamma)$, and overlaps considerably with the cosmological MDM favored region! The corresponding excluded regions from the false vacuum constraint [6] and $B(b \to s\gamma)$ for the m_0 *vs.* A_0 plane for $m_{1/2} = 200$ GeV are shown in Fig. 7.

C. Implications for Collider Experiments

Next, we wish to draw some conclusions for future searches for mSUGRA at colliding beam experiments. Expectations for mSUGRA in the same m_0 *vs.* $m_{1/2}$ planes have been worked out for the CERN LEP2 e^+e^- collider [26], various Fermilab Tevatron $p\bar{p}$ collider options [27], and for the CERN Large Hadron Collider (LHC) [28], a pp collider expected to operate at 14 TeV.

We return attention to Fig. 6*a*. If the mSUGRA model represents nature with parameters as in Fig. 6*a*, then the $B(b \to s\gamma)$ exclusion region wipes out most of the parameter space accessible to LEP2 SUSY searches. There are two exceptions [26]. There is a small region with $m_0 \gtrsim 200$ GeV and $m_{1/2} \simeq 100$ GeV where charginos could be accessible to LEP2 operating around $\sqrt{s} \sim 190$ GeV. In this region, the lightest neutralino $\widetilde{Z}_1$ can still be a good CDM candidate, since $m_{\widetilde{Z}_1} \sim \frac{M_Z}{2}$– thus, relic neutralinos can annihilate away via a Z boson pole in the s-channel. The other possibility for LEP2 is to discover a light Higgs boson h in the region beyond the $B(b \to s\gamma)$ exclusion contour. Much of the discovery reach of the Fermilab Main Injector ($\int \mathcal{L}dt = 2$ fb^{-1}) upgrade is also wiped out by the $b \to s\gamma$ constraint for the region $m_0 \lesssim 180$ GeV. As with LEP2, there is some remaining region of accessibility for seeing clean trileptons from $\widetilde{W}_1\widetilde{Z}_2 \to 3\ell$ around $m_0 \gtrsim 200$ GeV and $m_{1/2} \sim 120$ GeV. The TeV33 upgrade would be able to see in addition a large slice of parameter space beyond

the $b \to s\gamma$ excluded region up to $m_{1/2} \sim 275$ GeV for $m_0 \lesssim 100$ GeV, again via clean trileptons [27]. LHC would of course be able to scan well beyond the entire plane shown, up to values of $m_{1/2} \sim 700 - 1000$ GeV with just 10 fb^{-1} of data. Since $B(b \to s\gamma)$ decreases with increasing $m_{1/2}$ and m_0, however, the CLEO data prefer the region of parameter space accessible to LHC experiments, rather than the regions accessible to LEP2 and Tevatron, in contrast to preferences from fine-tuning [25].

Fig. 6*b* is entirely unconstrained by $B(b \to s\gamma)$. However, we do note that in this case the $B(b \to s\gamma)$ rate decreases with decreasing $m_{1/2}$ in the low $m_{1/2}$ region. Hence, the CLEO data actually *prefer* the regions accessible to LEP2 and Tevatron experiments, as do fine-tuning calculations.

For Fig. 6*c*, most of the plane shown is excluded by $B(b \to s\gamma)$, so if nature chose these parameters, then LEP2 and Tevatron upgrades would see nothing, and the discovery of SUSY would have to wait for LHC, which could access the very heavy sparticle spectra that lie at parameter space points beyond $m_{1/2} \sim 350$ GeV.

The parameter space of frame 6*d* is entirely allowed by $B(b \to s\gamma)$, and in fact the CLEO central value actually agrees with the parameter space region around $m_{1/2} \sim 200$ GeV. Since $B(b \to s\gamma)$ is decreasing below the SM value with decreasing $m_{1/2}$, the low $m_{1/2}$ region accessible to LEP2 and Tevatron upgrades is dis-favored by data. The region around $m_0 \sim 125$ and $m_{1/2} \sim 200$ is favored by $B(b \to s\gamma)$ and by cosmology, and has no non-standard minima in the scalar potential. In this favored region, unfortunately, neither SUSY nor Higgs particles would be accessible to LEP2 experiments. Only a fraction of this region would be accessible to Tevatron upgrades via trilepton searches. However, the CERN LHC would enjoy huge supersymmetric signal rates in this region, and in addition, direct production of sleptons would be visible as well.

IV. CONCLUSIONS

We have performed a calculation of $B(b \to s\gamma)$ as a function of the parameter space of the mSUGRA model. In doing so, we have included several improvements over the usual leading-log treatment. We have included corrections to the Wilson coefficients due to multiple scales in both the SUSY and SM loop contributions. We have also included the published NLO terms in the ADM elements needed for running the Wilson coefficients from a scale $Q = M_W$ down to $Q \sim m_b$. We have not included the correction to γ_{27}, so that our final result is not NLL. Preliminary results from the three loop calculation of $\gamma_{27}^{(1)}$ indicate it is only a small effect. Finally, we have included the virtual and bremsstrahlung graphs in the evaluation of the $< s\gamma|O_i|b >$ matrix elements. The combination of all the above elements leads to a $B(b \to s\gamma)$ calculation with reduced uncertainty due to choice of scale.

We plot our results as a function of mSUGRA model parameter space, and compare against recent results from the CLEO experiment. The comparison leads to allowed and excluded regions of mSUGRA parameter space. In particular, we note that for some mSUGRA parameter choices, the mSUGRA $B(b \to s\gamma)$ prediction agrees better than the SM one. The resulting constraints on parameter space are very strong, and indicate that large regions for $\mu < 0$ and for large $\tan\beta$ are excluded. We compare briefly with expectations for collider experiments at LEP2, Fermilab Tevatron, and CERN LHC. The $B(b \to s\gamma)$ constraint rules out much of parameter space that would have been accessible to LEP2 and Tevatron exper-

iments. However, we note that the region of parameter space most favored by $B(b \to s\gamma)$, cosmology and standard minima of the scalar potential, around $m_0 \sim 125$ GeV, $m_{1/2} \sim 200$ GeV, $\tan\beta \sim 10$ and $\mu > 0$ might be accessible to Fermilab MI or TeV33 searches for clean trileptons; if not, the discovery of SUSY would have to wait until LHC experiments are performed.

ACKNOWLEDGMENTS

We thank J. Hewett and X. Tata for discussions. In addition, we thank Manuel Drees for calculational comparisons which led to discovery of a bug in the program used to generate results for an earlier version of this manuscript. This research was supported in part by the U. S. Department of Energy under grant number DE-FG-05-87ER40319.

REFERENCES

[1] See, *e.g.* H. Haber in *Woodlands Superworld*, hep-ph/9308209 (1993).

[2] See *e.g.* M. Drees and S. Martin in *Electroweak Symmetry Breaking and New Physics at the TeV Scale*, edited by T. Barklow, S. Dawson, H . Haber and J. Seigrist, (World Scientific) 1995; see also J. Amundson *et. al.*, hep-ph/9609374 (1996).

[3] A. Chamseddine, R. Arnowitt and P. Nath, Phys. Rev. Lett. **49**, 970 (1982); R. Barbieri, S. Ferrara and C. Savoy, Phys. Lett. **B119**, 343 (1982); L.J. Hall, J. Lykken and S. Weinberg, Phys. Rev. **D27**, 2359 (1983).

[4] R. Cavanaugh (ALEPH Collaboration), seminar at Florida State University on *New Results from LEP2*, September, 1996.

[5] For a recent review, see G. Jungman, M. Kamionkowski and K. Griest, Phys. Rep. **267**, 195 (1996). See also M. Drees and M. Nojiri, Phys. Rev. **D47**, 376 (1993). The result shown here are from H. Baer and M. Brhlik, Phys. Rev. **D53**, 597 (1996). Further references are included in these reports.

[6] J. A. Casas, A. Lleyda and C. Mũnoz, Nucl. Phys. B**471**, 3 (1996); H. Baer, M. Brhlik and D. Castaño, Phys. Rev. D. (in press), hep-ph/9607465 (1996).

[7] See talk by J. Hewett presented at SLAC Summer Inst. on Particle Physics, SLAC-PUB-6521 (1993), hep-ph/9406302.

[8] M. S. Alam *et. al.*, (CLEO Collaboration), Phys. Rev. Lett. **74**, 2885 (1995).

[9] B. Grinstein, R. Springer and M. Wise, Nucl. Phys. B**339**, 269 (1989); J. Hewett, Phys. Rev. Lett. **70**, 1045 (1993); V. Barger, M. Berger and R. Phillips, Phys. Rev. Lett. **70**, 1368 (1993); M. Diaz, Phys. Lett. B**304**, 278 (1993); N. Deshpande, K. Panose and J. Trampetic, Phys. Lett. B**308**, 322 (1993).

[10] S. Bertolini, F. Borzumati, A. Masiero and G. Ridolfi, Nucl. Phys. B**353**, 591 (1991).

[11] R. Barbieri and G. F. Giudice, Phys. Lett. B**309**, 86 (1993); J. Lopez, D. Nanopoulos and G. Park, Phys. Rev. D**48**, 974 (1993); N. Oshimo, Nucl. Phys. B**404**, 20 (1993); R. Garisto and J. Ng, Phys. Lett. B**315**, 372 (1993); M. Diaz, Phys. Lett. B**322**, 207 (1994); Y. Okada, Phys. Lett. B**315**, 119 (1993); F. Borzumati, Zeit. für Physik C**63**, 291 (1994); P. Nath and R. Arnowitt, Phys. Lett. B**336**, 395 (1994); G. Kane, C. Kolda, L. Roszkowski and J. Wells, Phys. Rev. D**49**, 6173 (1994); F. Borzumati, M. Drees and M. Nojiri, Phys. Rev. D**51**, 341 (1995); V. Barger, M. Berger, P. Ohmann and R. Phillips, Phys. Rev. D**51**, 2438 (1995); F. Bertolini and F. Vissani, Zeit. für Physik C**67**, 513 (1995); J. Lopez, D. Nanopoulos, X. Wang and A. Zichichi, Phys. Rev. D**51**, 147 (1995); J. Wu, R. Arnowitt and P. Nath, Phys. Rev. D**51**, 1371 (1995); B. de Carlos and J. A. Casas, Phys. Lett. B**349**, 300 (1995) and ERRATUM-*ibid* B**351**, 604 (1995).

[12] C. Greub and T. Hurth, SLAC-PUB-7267 (1996), hep-ph/9608449.

[13] M. A. Shifman, A. I. Vainshtein and V. I. Zacharov, Phys. Rev. D**18**, 2583 (1978); S. Bertolini, F. Borzumati and A. Masiero, Phys. Rev. Lett. **59**, 180 (1987); N. G. Deshpande, G. Eilam, P. Lo and J. Trampetic, Phys. Rev. Lett. **59**, 183 (1987); B. Grinstein, R. Springer and M. Wise, Phys. Lett. B**202**, 138 (1988); R. Grigjanis, P. J. O'Donnel and M. Sutherland, Phys. Lett. B**213**, 355 (1988) and Phys. Lett. B**224**, 209 (1989); G. Cella, G. Curci, G. Ricciardi and A. Vicere, Phys. Lett. B**248**, 181 (1990); M. Misiak, Phys. Lett. B**269**, 161 (1991) and Nucl. Phys. B**393**, 23 (1993); M. Ciuchini, E. Franco, G. Martinelli, L. Reina and L. Silvestrini, Phys. Lett. B**316**, 127 (1993); M. Ciuchini, E. Franco, L. Reina and L. Silvestrini, Nucl. Phys. B**421**, 41 (1993).

[14] A. J. Buras, M. Misiak, M. Münz and S. Pokorski, Nucl. Phys. B**424**, 374 (1994).
[15] P. Cho and B. Grinstein, Nucl. Phys. B**365**, 279 (1991).
[16] H. Anlauf, Nucl. Phys. B**430**, 245 (1994).
[17] M. Ciuchini, E. Franco, G. Martinelli and L. Reina, Nucl. Phys. B**415**, 403 (1994).
[18] M. Misiak and M. Münz, Phys. Lett. B**344**, 308 (1995).
[19] K. G. Chetyrkin, M. Misiak and M. Münz, in preparation; talk given by M. Misiak at ICHEP96, Warsaw, Poland, July, 1996.
[20] J. M. Soares, Phys. Rev. D**49**, 283 (1994).
[21] C. Greub, T. Hurth and D. Wyler, Phys. Lett. B**380**, 385 (1996) and Phys. Rev. D**54**, 3350 (1996).
[22] A. Ali and C. Greub, Z. Phys. C**49**, 431 (1991), Phys. Lett. B**259**, 182 (1991), **287**, 191 (1992) and **361**, 146 (1995); Z. Phys. C**60**, 433 (1993); N. Pott, Phys. Rev. D**54**, 938 (1996);
[23] H. Baer, C. H. Chen, R. Munroe, F. Paige and X. Tata, Phys. Rev. D**51**, 1046 (1995).
[24] For discussion, see N.G. Deshpande, X. G. He and J. Trampetic, Phys. Lett. **B367**, 362 (1996).
[25] G. Anderson and D. Castaño, Phys. Rev. D**53**, 2403 (1995).
[26] H. Baer, M. Brhlik, R. Munroe and X. Tata, Phys. Rev. D**52**, 5031 (1995).
[27] H. Baer, C. H. Chen, C. Kao and X. Tata, Phys. Rev. D**52**, 1565 (1995); H. Baer, C. H. Chen, F. Paige and X. Tata, Phys. Rev. D (in press).
[28] H. Baer, C. H. Chen, F. Paige and X. Tata, Phys. Rev. D**52**, 2746 (1995) and Phys. Rev. D**53**, 6241 (1996).

FIGURES

FIG. 1. We plot the value of the Wilson coefficient $C_7(M_W)$ versus $m_{1/2}$, where $m_0 = m_{1/2}$, $\tan\beta = 2$, $A_0 = 0$. In *a*), we take $\mu < 0$ and in *b*) we take $\mu > 0$. The various loop contributions to $C_7(M_W)$ are denoted on the plot. The label $\tilde{q}$ refers to the sum over $\tilde{q} = \tilde{u}_L, \tilde{u}_R, \tilde{c}_L, \tilde{c}_R$ contributions.

FIG. 2. Evolution of Wilson coefficients $C_i(Q)$ for $i = 1 - 8$ from $Q = M_W$ to $Q = 1$ GeV, for $(m_0, m_{1/2}, A_0, \tan\beta, sign(\mu) = (100, 100, 0, 10, -1)$, where masses are in GeV units. Frame *a*) shows evolution to LO, while frame *b*) shows NLO evolution (except $\gamma_{27}^{(1)} = 0$).

FIG. 3. A plot of the SM branching ratio $B(b \to s\gamma)$ versus scale choice Q, where $\frac{m_b}{2} < Q < 2m_b$. We plot the LL result, and in addition, our QCD-improved result. The theoretical error diminishes from $\sim 25\%$ to $\sim 9\%$. We also plot the CLEO measured central value, as well as 1σ and 95% CL limits on the experimental result.

FIG. 4. Plot of contours of constant branching ratio $B(b \to s\gamma)$ in the m_0 *vs.* $m_{1/2}$ plane, where $A_0 = 0$ and $m_t = 170$ GeV. Each contour should be multiplied by 10^{-4}. Frame *a*) is for $\tan\beta = 2,\ \mu < 0,$ *b*) is for $\tan\beta = 2,\ \mu > 0,$ *c*) is for $\tan\beta = 10,\ \mu < 0$ and *d*) is for $\tan\beta = 10,\ \mu > 0$. The regions labelled by TH (EX) are excluded by theoretical (experimental) considerations. The dashed contour corresponds to the latest LEP2 limit of $m_{\widetilde{W}_1} > 79$ GeV for a gaugino-like chargino.

FIG. 5. Plot of contours of constant branching ratio $B(b \to s\gamma)$ in the m_0 *vs.* A_0 plane, where $m_{1/2} = 200$ GeV and $m_t = 170$ GeV. Each contour should be multiplied by 10^{-4}. Frame *a*) is for $\tan\beta = 2,\ \mu < 0,$ *b*) is for $\tan\beta = 2,\ \mu > 0,$ *c*) is for $\tan\beta = 10,\ \mu < 0$ and *d*) is for $\tan\beta = 10,\ \mu > 0$. The regions labelled by TH (EX) are excluded by theoretical (experimental) considerations.

FIG. 6. Plot of contours of various constraints on the mSUGRA model in the m_0 *vs.* $m_{1/2}$ plane, where $A_0 = 0$ and $m_t = 170$ GeV. The frames are as in Fig. 4. To the left of the contour marked by open circles is the region where minima occur in the mSUGRA scalar potential that are deeper than the standard one. The region below the dashed contour is excluded by the LEP2 limit that $m_{\widetilde{W}_1} > 79$ GeV. The region to the right of the solid contour labelled Ωh^2 is excluded because the universe would be younger than 10 billion years old ($\Omega h^2 > 1$). The region between the dot-dashed contours is favored by the cosmological mixed dark matter scenario, where $0.15 < \Omega h^2 < 0.4$. Finally, the region to the lower-left of the solid contour labelled $b \to s\gamma$ in frame *a*) is excluded at 95% CL by the analysis of this paper. The entire region in frame *b*) is allowed by $b \to s\gamma$, while almost the entire region in frame *c*) is excluded by $b \to s\gamma$. Finally, the entire region shown in frame *d*) is again allowed by the $b \to s\gamma$ constraint.

FIG. 7. Plot of contours of various constraints on the mSUGRA model in the m_0 *vs.* A_0 plane, where $m_{1/2} = 200$ GeV and $m_t = 170$ GeV. The frames are as in Fig. 5. To the left of the contour marked by open circles is the region where minima occur in the mSUGRA scalar potential that are deeper than the standard one. The entire regions in frames *a*), *b*) and *d*) are allowed by $b \to s\gamma$, while the entire region in frame *c*) is excluded by $b \to s\gamma$.

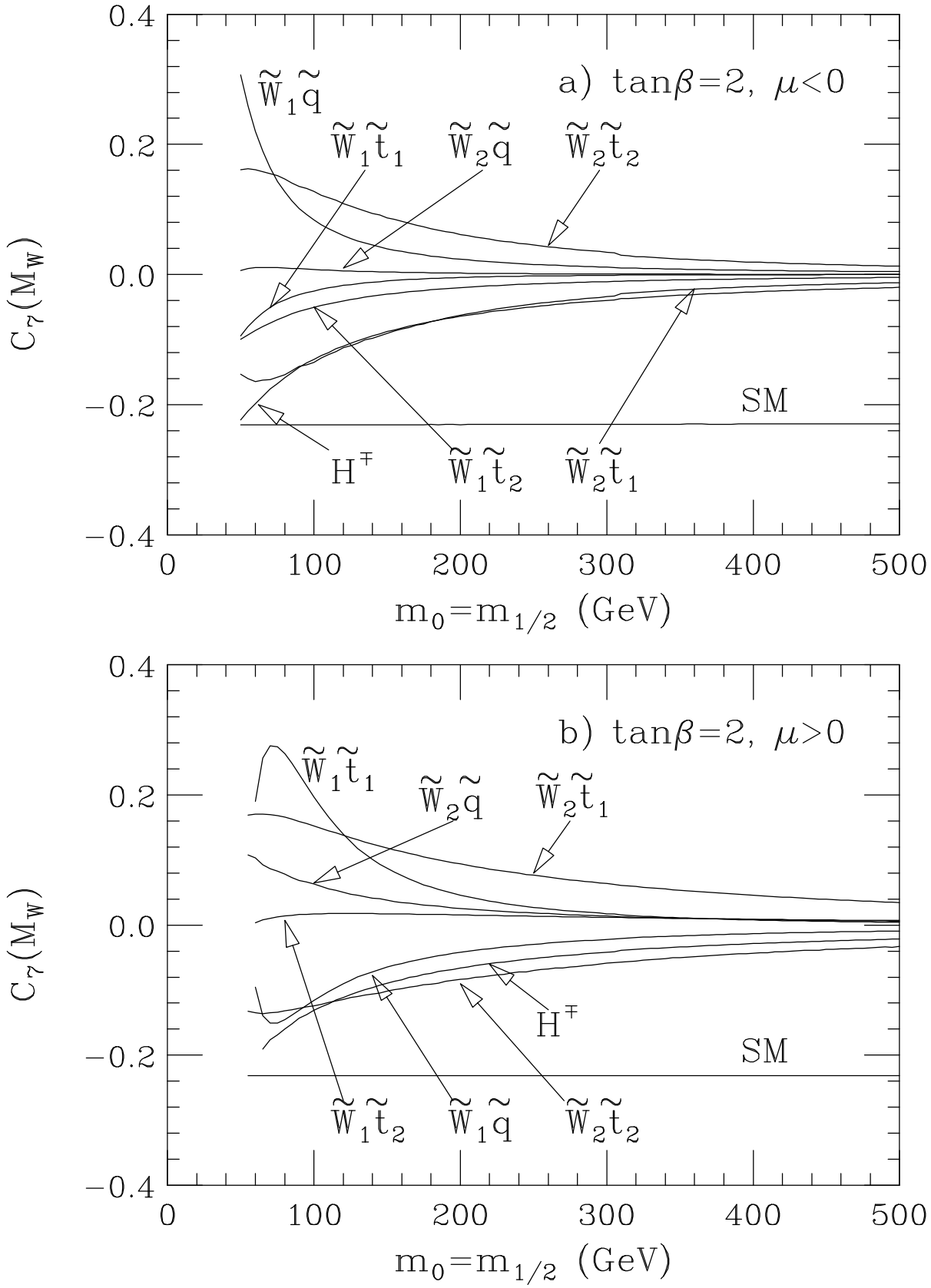
a) tanβ=2, μ<0
b) tanβ=2, μ>0
$\tilde{W}_1\tilde{q}$
$\tilde{W}_1\tilde{t}_1$
$\tilde{W}_2\tilde{q}$
$\tilde{W}_2\tilde{t}_2$
$H^{\mp}$
$\tilde{W}_1\tilde{t}_2$
$\tilde{W}_2\tilde{t}_1$
SM
$C_7(M_W)$
$m_0=m_{1/2}$ (GeV)
0.4
0.2
0.0
−0.2
−0.4
0
100
200
300
400
500

Fig. 1

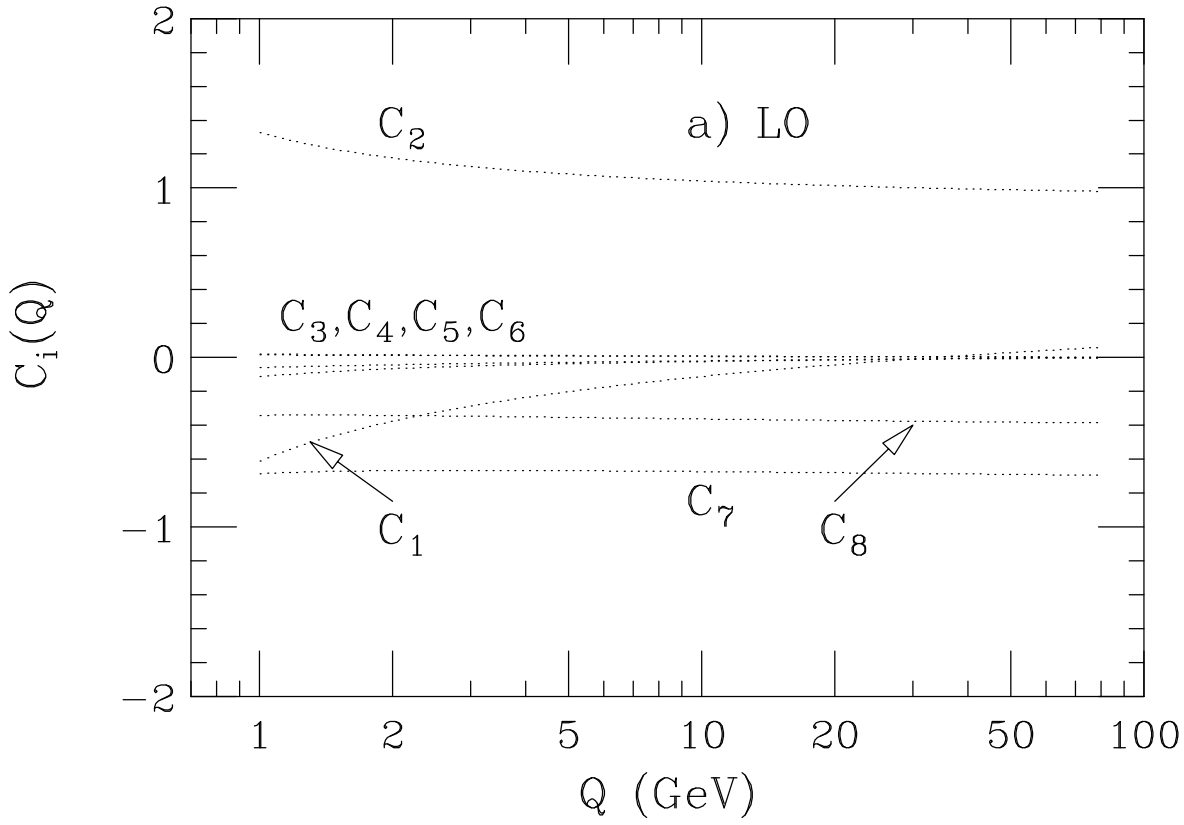
a) LO
C_2
C_3, C_4, C_5, C_6
C_1
C_7
C_8
$C_i(Q)$
Q (GeV)
2
1
0
−1
−2
1
2
5
10
20
50
100

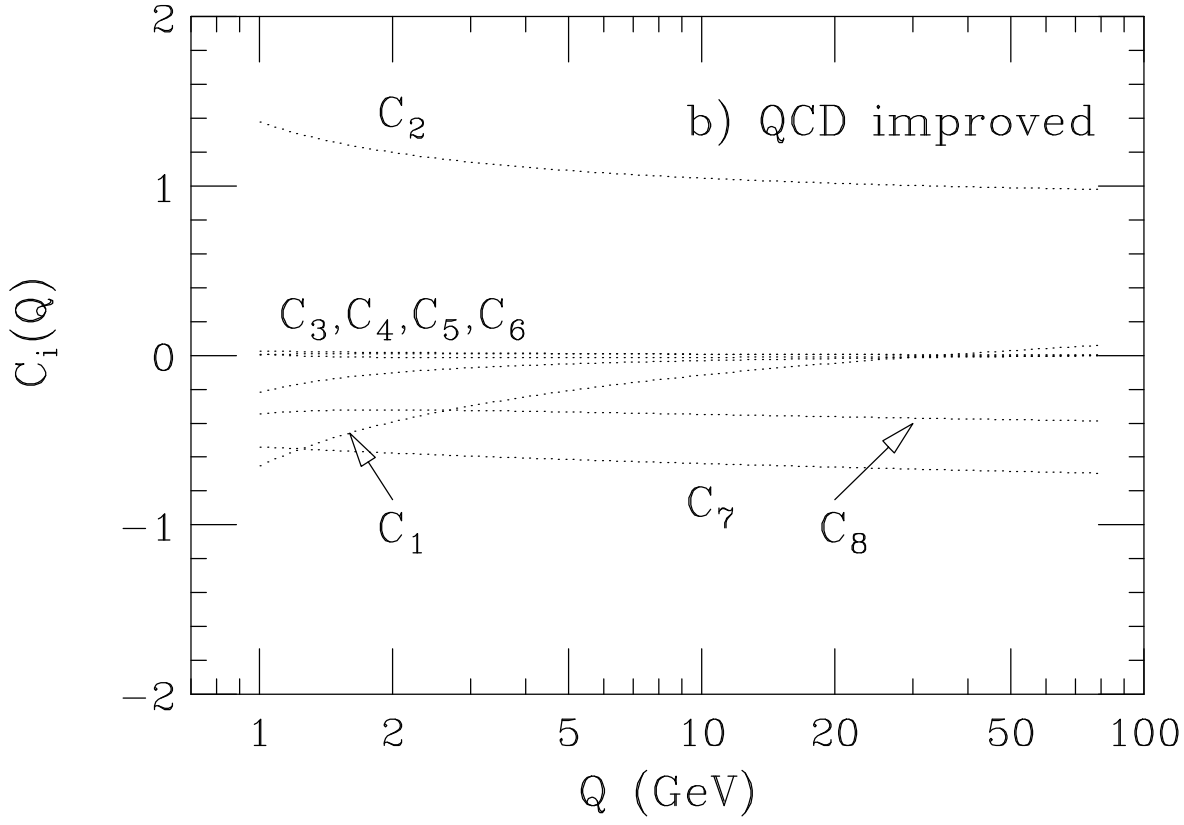
b) QCD improved
C_2
C_3, C_4, C_5, C_6
C_1
C_7
C_8
$C_i(Q)$
Q (GeV)
2
1
0
−1
−2
1
2
5
10
20
50
100

Fig. 2

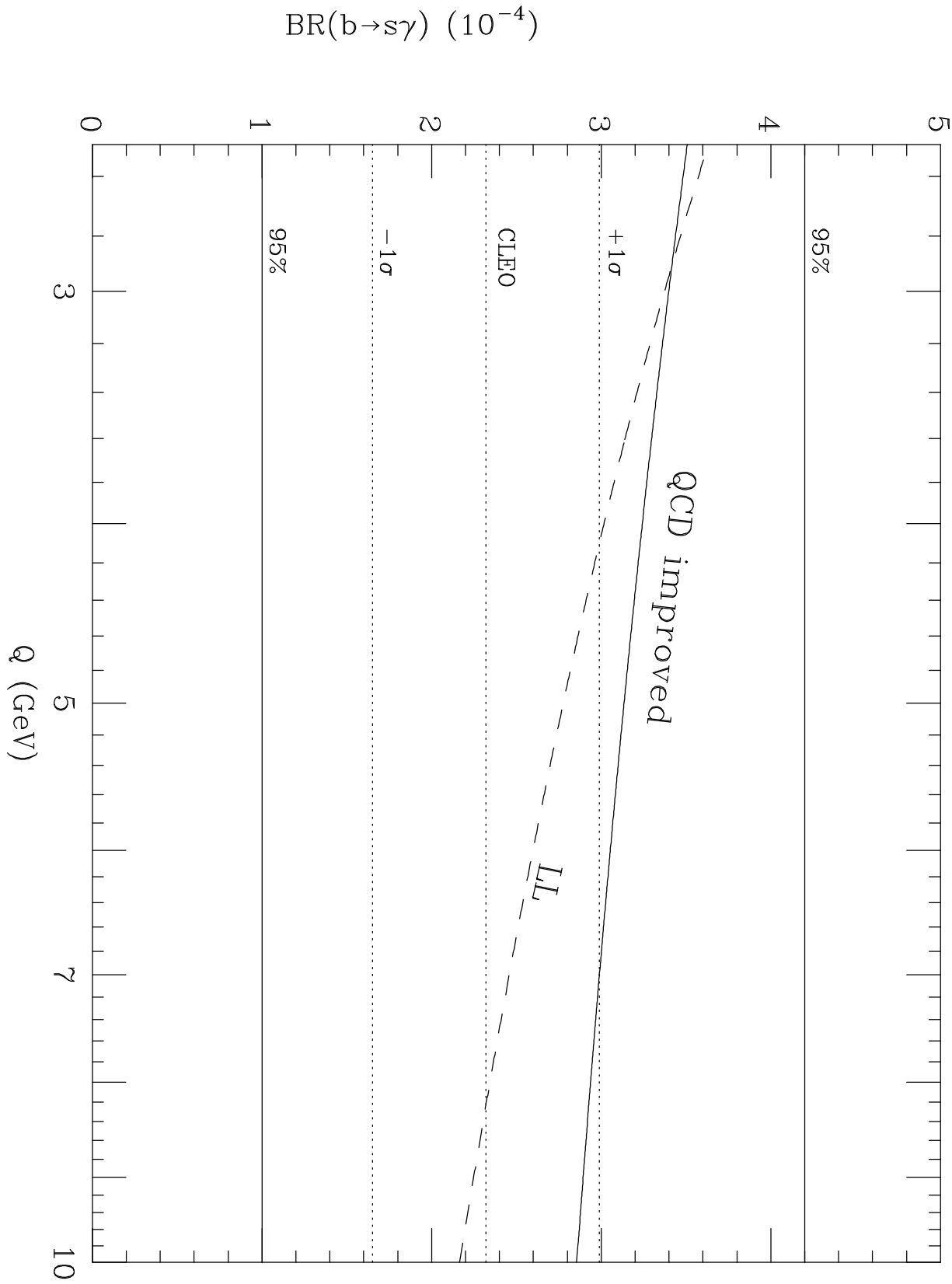

Fig. 3

a) tanβ=2
A0=0; μ<0
b) tanβ=2
A0=0; μ>0
c) tanβ=10
A0=0; μ<0
d) tanβ=10
A0=0; μ>0
m1/2 (GeV)
m0 (GeV)
TH
EX
0
100
200
300
400
500
5.
4.5
4.
3.5
3.4
3.3
3.2
3.1
3.
10.
8.
6.
4.
2.5
2.
1.5

Fig. 4

a) tanβ=2
m1/2=200
μ<0
b) tanβ=2
m1/2=200
μ>0
c) tanβ=10
m1/2=200
μ<0
d) tanβ=10
m1/2=200
μ>0
TH
A0 (GeV)
m0 (GeV)
4.2
3.8
3.6
3.4
3.2
3.
7.
6.
5.
2.5
2.
1.5

Fig. 5

a) tanβ=2
A0=0; μ<0
Ωh²
b→sγ
TH
EX
b) tanβ=2
A0=0; μ>0
allowed
c) tanβ=10
A0=0; μ<0
d) tanβ=10
A0=0; μ>0
m1/2 (GeV)
m0 (GeV)
0
100
200
300
400
500

Fig. 6

A0 (GeV)
m0 (GeV)
a) tanβ=2
m1/2=200
μ<0
allowed
TH
b) tanβ=2
m1/2=200
μ>0
allowed
TH
c) tanβ=10
m1/2=200
μ<0
excluded
d) tanβ=10
m1/2=200
μ>0
allowed

Fig. 7